Coherent and thermal light: Tunable hybrid states with second-order coherence without first-order coherence

Martin Blazek[*] and Wolfgang Elsäßer[†]

Institute of Applied Physics, Technische Universität Darmstadt, Schlossgartenstrasse 7, D-64289 Darmstadt, Germany

(Received 1 July 2011; published 19 December 2011)

We demonstrate the realization of a new hybrid state of light that is simultaneously spectrally broadband, i.e., in-coherent in first order, and exhibits a laserlike normalized intensity correlation coefficient of 1.33, reflecting high coherence in second order. This is achieved by temperature-tuned light emission from an optoelectronic quantum dot superluminescent diode where the condensation of injected charge carriers into the globally lowest energy state of the strongly inhomogeneously broadened semiconductor quantum dot ensemble gives rise to a particular balance between spontaneous and stimulated emission.

DOI: 10.1103/PhysRevA.84.063840 PACS number(s): 42.50.Gy, 32.80.Qk, 78.67.Hc

I. INTRODUCTION

The coherence properties of photonic beams are governed by the nature of the photon emission process. In contrast to fully coherent laser light originating from stimulated emission events, thermal light generated by spontaneous emission is incoherent in first and second order, where first-order coherence characterizes the correlations of the field depending on the spectral bandwidth of the source [1] and second-order coherence is related to intensity correlations reflecting the temporal distribution of photons [2]. An exciting photon state with interesting coherence properties is realized by amplified spontaneous emission (ASE), which contains ingredients from both spontaneous and stimulated emission [3].

Electrically pumped superluminescent diodes (SLD's) that unite the spatially narrow output beam of a laser with the spectrally broadband character of an LED are an efficient and compact source of ASE light on a semiconductor basis [4]. This unique combination is achieved by a tilted waveguide design with antireflection-coated facets that suppresses modal laser emission and leads to a smooth optical output spectrum that is determined by the gain curve of the active material. Various optical properties can be tailored by the proper choice of the gain material, and even further control of the emission parameters can be achieved by nanostructuring the active region [5–8] where in the final step carriers are confined in tiny pyramids [9], the so-called quantum dots (QD's). Similar to atoms, optoelectronic QD's represent fully quantized zero-dimensional carrier systems with particularly interesting energy level schemes. An electron that is injected into a dot can recombine with a hole under the emission of radiation. The lowest optical transition inside each dot is commonly referred to as the ground state (GS), which is followed by the first excited state (ES) and second excited state (SES) at higher energies [see Fig. 1(a)]. The exact position of the energy levels within each dot, and therefore the photon energy, is determined by a variety of intrinsic dot parameters, e.g., material, composition, size, and shape [10], which complement variations of the band gap induced by temperature changes [11]. Spectrally broadband emission is finally achieved through a self-organized growth process that introduces large dot size variations in the ensemble resulting in a strong inhomogeneous broadening of all optical transitions [12] leading to a short coherence length in first order.

The coherence properties in second order can be described by the normalized second-order correlation function $g^{(2)}(\tau) = \langle I(t)^* I(t+\tau)\rangle / \langle I(t)\rangle^2$, where the correlation of field intensity $I(t)$ is performed at different time delays τ and $\langle\ \rangle$ designates statistical averaging [13]. With the advent of quantum optics, accompanied by the famous Hanbury-Brown and Twiss experiment, there has always been the paradigm that a monochromatic laser emits photons with an intensity correlation of $g^{(2)}(\tau) = 1$ reflecting Poissonian photon statistics, whereas spectrally broadband incoherent light from a thermal source exhibits an enhanced intensity correlation of $g^{(2)}(\tau = 0) = 2$ at zero time delay, inevitably connected to photon bunching [14,15]. In this article, we break this paradigm and demonstrate simultaneously spectrally broadband emission in the near-infrared spectral region with an optical bandwidth of several THz and laserlike intensity correlations of 1.33 by controlling the photon emission process in a QD SLD through a temperature-induced occupation condensation of the injected charge carriers. This coherent and thermal light with tunable hybrid coherence properties represents an exciting new class of classical photon states that not only stimulates perpetual scientific interest in the quantum nature of light, as in the very recent field of "ghost imaging" [16,17] where correlations and spectral properties play a key role, but also represents an ideal, intensity-stabilized light source for low-coherent light applications such as optical coherence tomography [18].

II. EXPERIMENTAL RESULTS

The investigated SLD consists of six active layers containing InAs dots embedded in InGaAs quantum wells (QW's). We analyze the coherence properties of the SLD emission through photon correlation studies [19] with a time resolution shorter than the coherence time [20] of the SLD, which is in the order of femtoseconds. We apply an appropriate experimental technique that has recently been demonstrated by Boitier *et al.* [21], where they succeeded in measuring $g^{(2)}(\tau)$ of thermal light by exploiting the effect of two-photon absorption (TPA)

[*]martin.blazek@physik.tu-darmstadt.de

[†]Also with Center of Smart Interfaces, Technische Universität Darmstadt, Petersenstrasse 32, D-64287 Darmstadt, Germany.

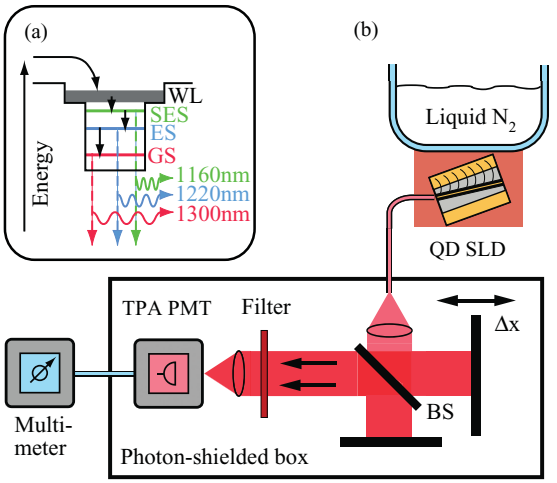

FIG. 1. (Color online) (a) Single quantum dot energy level scheme. Carriers enter the ground-state (GS), excited-state (ES), and second-excited-state (SES) optical transitions through the wetting layer (WL) and recombine with the emission of photons. For low pump currents, only the GS transition emits. With increasing current, the ES and SES transitions also contribute to the emission. (b) Two-photon absorption setup. The QD SLD is operated inside a liquid-nitrogen-cooled cryostat. The emission enters the Michelson interferometer consisting of a beamsplitter, BS, a fixed and a variable mirror with the displacement, Δx. The combined beams pass a long-pass filter ($\lambda > 850$ nm) and are tightly focused onto the photomultiplier tube (PMT) where the TPA signal is generated.

[22,23] in a semiconductor GaAs photomultiplier tube. To investigate the temperature dependence of $g^{(2)}(\tau)$, we operate the QD SLD inside a liquid-nitrogen-cooled cryostat where the temperature could be varied from 290 down to 90 K [Fig. 1(b)]. The nonlinear TPA signal is generated by tightly focusing the SLD emission onto a Hamamatsu R928 photomultiplier tube (PMT) that operates in TPA mode at the output of a Michelson interferometer. The characteristic signature of TPA processes given by the quadratic relation of PMT current to optical input power has been verified for the investigated power regime. To correlate photons at different time delays τ, one mirror of the interferometer is mounted on a high-precision translation stage. We record the PMT current as a function of mirror displacement and extract $g^{(2)}(\tau)$ analogous to Refs. [21,24] by applying a low pass filter and normalizing the interferogram to the sum of the individual PMT currents with one path of the interferometer blocked, respectively.

The temperature dependence of the spectral properties of the QD SLDs' emission is discussed exemplarily by means of three optical output spectra at 290, 190, and 90 K. At room temperature and a constant pump current of 1 A, the QD SLD emits amplified spontaneous emission with an optical spectrum that is dominated by the ES contribution at 1.22 μm exhibiting a broad spectral bandwidth of 35 nm or 8 THz (Fig. 2). The temperature-induced changes in the optical spectra reflecting the band-gap variations lead to an overall blueshift of the entire emission spectrum that is complemented by a relative change in the intensity ratio of the contributing GS and ES transitions, such that the ES-dominated emission at room temperature develops continuously into a GS-dominated

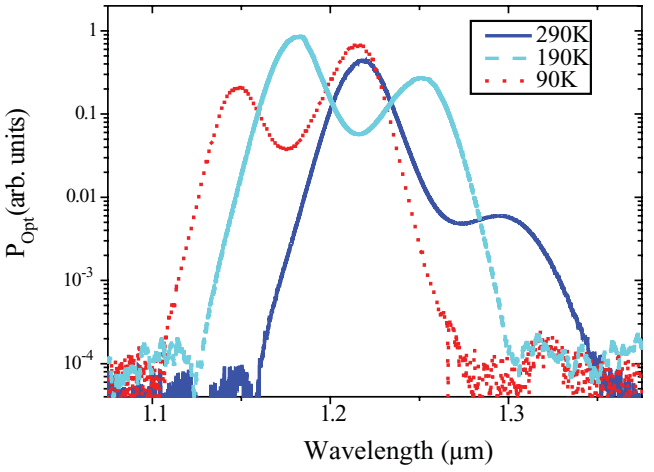

FIG. 2. (Color online) Optical spectra of QD SLD at a pump current of 1 A for various temperatures. With reducing temperature, the optical spectra shift to shorter wavelengths and the relative intensity changes from an ES-dominated emission at 290 K to a GS-dominated emission at 90 K.

emission at 90 K. The origin of this temperature-induced spectral dynamic is discussed below. With decreasing temperature, the output power of the total emission increases. Compared to room-temperature operation, the output powers at 190 and 90 K experience a 2.5- and 1.8-fold increase, respectively.

For room-temperature operation of the SLD, the interferogram, containing both first- and second-order coherence properties, is shown in Fig. 3(a) together with $g^{(2)}(\tau)$. In the interferogram, bright and dark fringes alternate with a period corresponding to the SLD's central emission wavelength of

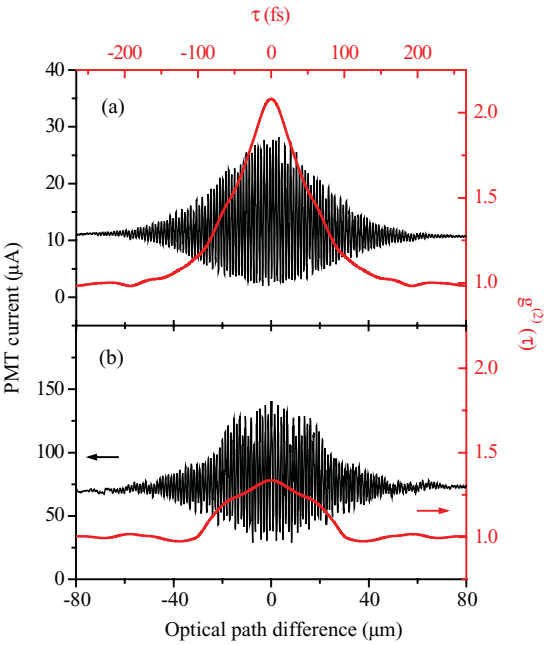

FIG. 3. (Color online) SLD coherence properties. (a) TPA interferogram (left scale) and second-order coherence function $g^{(2)}(\tau)$ (right scale) at 290 K, with $g^{(2)}(0) = 2.04 \pm 0.05$ indicating the photon bunching. (b) TPA interferogram at 190 K, with $g^{(2)}(0) = 1.33 \pm 0.05$ indicating a more regular photon emission.

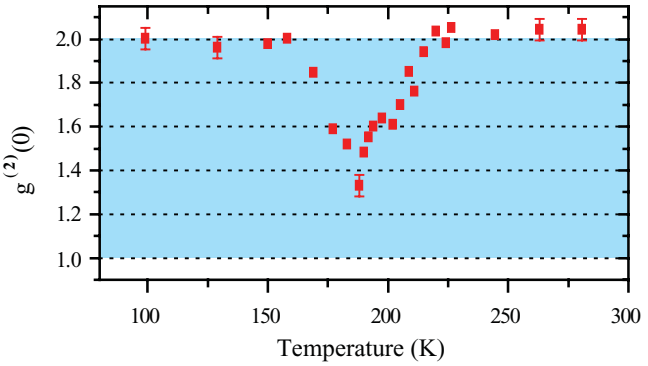

FIG. 4. (Color online) Reduced photon bunching. Second-order correlation coefficient $g^{(2)}(0)$ at various temperatures. Error bars are shown exemplarily. The limiting cases of fully coherent laser emission reflected by $g^{(2)}(0) = 1$ and totally incoherent thermal emission with $g^{(2)}(0) = 2$ confine the shaded region.

1.22 μm. The contrast of the fringes quickly vanishes for optical path differences exceeding 60 μm ($\tau > 200$ fs) reflecting the SLD's short coherence length of only 32 μm. We find a value of $g^{(2)}(\tau = 0) = 2.04 \pm 0.05$ for equal optical path lengths, indicating an enhanced probability of detecting two photons simultaneously, the direct manifestation of photon bunching. At room temperature, the amplified spontaneous emission of the QD SLD, therefore, represents "pure" first- and second-order broadband incoherent thermal light with photon bunching and large intensity fluctuations [25]. The observed value of $g^{(2)}(0) = 2$ clearly differs from $g^{(2)}(0) = 1$, which is expected for coherent laser emission and represents the ultimate limit in the classical description of light [26,27]. A modification of $g^{(2)}(0)$ toward 1, therefore, reflects a higher degree of second-order coherence [19]. However, an even more regular, "fermionic" photon distribution can be achieved by nonclassical light sources that exhibit antibunching [28] with $g^{(2)}(\tau)$ values smaller than 1. Note that the ratio between the central and the decorrelated part of the PMT current at large time delays does not reach the ideal 1:4 ratio that is obtained in [21]. We attribute this reduction to mechanical vibrations that occur during the scanning process and partially anticipate the low-pass filtering procedure.

III. HYBRID-COHERENT LIGHT GENERATION

Now we analyze the temperature dependence of the coherence properties, where $g^{(2)}(0)$ represents an indicator for the magnitude of photon bunching (Fig. 4). Starting with $g^{(2)}(0) \sim 2$ at room temperature, we find a decreasing behavior with a pronounced minimum of $g^{(2)}(0) = 1.33 \pm 0.05$ at 190 K. For lower temperatures, $g^{(2)}(0)$ tends toward 2 again. Transferred to the photon picture, the striking reduction of $g^{(2)}(0)$ down to 1.33 means that the groups of photons break up and the photon stream becomes more regular, shifting the temporal photon distribution toward that of a laser. In this "stabilized" emission regime with reduced fluctuations, we access an interesting class of hybrid photon states with still low first-order coherence and increased second-order coherence. As is evident from the fast decay of the interferogram in Fig. 3(b), the coherence length of the SLD equals 27 μm and remains almost unaffected by the temperature variation. The additional peaks in $g^{(2)}(\tau)$ at ± 60 fs, originating from the beating of spectral GS and ES components, are not responsible for the $g^{(2)}(0)$ reduction as they become even more pronounced at lower temperatures where $g^{(2)}(0)$ increases again.

Recently, a similar hybrid light state was realized in an SLD utilizing a quantum-well gain material [29]. However, there, by operating the QW SLD at high pump currents close to the lasing threshold, a different physical mechanism was responsible for the generation of spectrally broadband light with reduced intensity fluctuations. Here, in contrast, we exploit the unique properties of quantized zero-dimensional quantum dot charge-carrier systems to manipulate the delicate emission hierarchy balance between spontaneous and stimulated emission in the amplified spontaneous emission of the QD SLD by temperature tuning. Furthermore, regarding the achievable spectral bandwidth, QD gain materials can, via the balanced combination of GS and ES contributions, provide amplification over more than 100 nm [30] and thereby easily exceed the spectral range of QW SLD's.

IV. DISCUSSION

For the description of this temperature-dependent reduced second-order correlation coefficient, we now consult a rate equation model that has been developed previously to describe the threshold currents' temperature dependence of strongly inhomogeneously broadened quantum dot lasers reflecting its radiative recombination processes [31,32]. Thereby, we combine the two worlds of quantum optics and semiconductor quantum dots. The charge-carrier distribution in semiconductor QD materials depends on temperature, and the mean carrier occupation number for each energy level is obtained by averaging over the whole inhomogeneous dot ensemble. The ingredients of the model are the two confined quantum dot levels, namely the GS and the ES, and the so-called wetting layer, which provides the joint interaction medium for all quantum dots. Their appropriate interaction is accounted for by relaxation rates, carrier escape processes via thermally activated escape, tunneling, and Auger processes. Finally, all states interact with a Bose-Einstein phonon bath. The outcome is the carrier distribution or the population densities entering directly the radiative photon emission rates. At room temperature, high-energy phonons induce a global thermal equilibrium of the whole QD ensemble through interaction with the surrounding wetting layer [Fig. 5(a), top] and thermally excite some of the carriers into higher energetic states, leaving some of the lower states unoccupied [Fig. 5(b), top] such that the occupation is described by an equilibrium Fermi-Dirac distribution with a global Fermi level for all electron levels. When the temperature is reduced, the carriers are still uniformly distributed among the individual dots. However, thermal excitations freeze out, the nonradiative losses decrease, and charge-carrier condensation into the globally lowest energy state occurs, thereby maximizing the occupation numbers of the GS and ES transitions [Figs. 5(a) and 5(b), middle]. At even lower temperatures, this common occupation statistics or global equilibrium collapses. The exchange of carriers between the individual dots breaks down, and inside each dot all the energetically lowest states have the same population irrespective of their energy, which

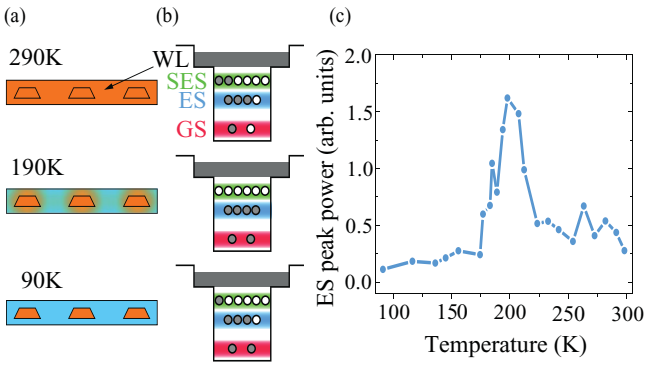

FIG. 5. (Color online) Charge-carrier condensation. (a) Schematic visualization of the thermal coupling of three identical quantum dots embedded in the wetting layer for various temperatures. Top: Strong coupling occurs at 290 K. Middle: Reduced thermal coupling at 190 K and thermally isolated dots at 90 K (bottom). (b) Mean carrier occupation per energy level averaged over the whole QD ensemble. Broadened bands are chosen to illustrate the inhomogeneous broadening of all levels. The number of available carrier sites increases for higher states due to an increased level degeneracy. Gray circles denote states occupied by carriers; white circles indicate empty states. At 190 K, charge-carrier condensation maximizes the excited-state occupation. (c) Excited-state spectral peak power with a local maximum close to 190 K.

characterizes a so-called random population. The resulting distribution is a nonequilibrium distribution with a "virtual" excitation spectrum obtained by averaging over the whole ensemble [Figs. 5(a) and 5(b), bottom], thus reflecting more the energetically inhomogeneous dot distribution. This leads again to a decrease in radiative recombination accompanied by a small increase in linewidth. In essence, at around 190 K, a maximum in the radiative recombination occurs due to the occupation condensation into the globally lowest-lying state that is still described by a Fermi-Dirac distribution.

This redistribution of carriers modifies the optical gain properties of the SLD that we investigate through temperature-resolved spectral analysis. The spectral peak power extracted from the maximum value of the optical spectra shown in Fig. 2 represents an easily accessible indicator for the spectral gain. The relative development of the spectral gain of the excited-state contribution that dominates the total emission down to temperatures of 160 K is shown in Fig. 5(c). In the weakly coupled thermal regime at 190 K, we find an increase by a factor of 6 in peak power compared to room temperature due to the condensation of charge carriers. The local maximum in peak power indicates a larger amplification, which in turn affects the photon emission process [3]. At room temperature, the QD SLD emits amplified spontaneous emission in a delicate balance, where spontaneously emitted photons are amplified moderately. At 190 K, the maximum in the spectral gain increases the probability of stimulated emission such that the initial spontaneous emission experiences a stronger amplification. These quasistimulated processes increase the second-order coherence and suppress intensity fluctuations [25,33], thus realizing the exciting hybrid coherent photon states. The intensity noise level of the QD SLD has been measured by the experimental technique of direct detection [29] in the white-noise-dominated frequency regime between 20 and 30 MHz. Compared to the noise level at room temperature (-130 dB/Hz), we found a beneficial intensity noise reduction of -13 dB/Hz for the hybrid coherently emitting QD SLD at 190 K. At lower temperatures, the gain of the ES contribution is reduced, and conventional incoherent ASE is again obtained. Of course, it is worthwhile to think of a further increase in the peak gain to reach the classical correlation limit of $g^{(2)}(0) = 1$. However, one has to be aware that the crucial requirements in the SLD design to prevent modal emission and therefore maintain low first-order coherence will become even more demanding.

V. CONCLUSION

In summary, we have shown that a temperature-induced increase of stimulated emission in QD SLD's creates second-order coherence and tears bunched thermal photons apart. The resulting new class of photon states with tunable hybrid coherence properties provides a deeper and more complete understanding of the light generation process and represents an ideal candidate for low-coherent light applications.

ACKNOWLEDGMENTS

The authors acknowledge device fabrication and processing from the University of Sheffield (M. Hopkinson) and Alcatel Thales III-V Labs (M. Krakowski) and experimental assistance from S. Hartmann. This work has been performed within the European Union funded STREP project NANO UB-SOURCES. We are grateful to an anonymous referee for pointing out and proving theoretically that other, completely different approaches may exist to break the "thermal-coherent" paradigm, however, with a moderately smaller spectral bandwidth on the order of MHz.

[1] A. Einstein, Arch. Sci. Phys. Nat. **37**, 254 (1914).
[2] L. Mandel and E. Wolf, *Selected Papers on Coherence and Fluctuations of Light* (Dover Publication Inc., New York, 1971).
[3] D. S. Wiersma, Nat. Phys. **4**, 359 (2008).
[4] T. P. Lee, C. A. Burrus, and B. I. Miller, IEEE J. Quantum Electron. **QE-9**, 820 (1973).
[5] Z. I. Alferov, Rev. Mod. Phys. **73**, 767 (2001).
[6] H. Kroemer, Rev. Mod. Phys. **73**, 783 (2001).
[7] S. M. Ulrich, C. Gies, S. Ates, J. Wiersig, S. Reitzenstein, C. Hofmann, A. Löffler, A. Forchel, F. Jahnke, and P. Michler, Phys. Rev. Lett. **98**, 043906 (2007).
[8] D. V. Regelmann, U. Mizrahi, D. Gershoni, E. Ehrenfreund, W. V. Schoenfeld, and P. M. Petroff, Phys. Rev. Lett. **87**, 257401 (2001).

[9] R. Dingle, A. C. Gossard, and W. Wiegmann, Phys. Rev. Lett. **34**, 1327 (1975).
[10] O. Stier, M. Grundmann, and D. Bimberg, Phys. Rev. B **59**, 5688 (1999).
[11] Y. T. Dai, J. C. Fan, Y. F. Chen, R. M. Lin, S. C. Lee, and H. H. Lin, J. Appl. Phys. **82**, 4489 (1997).
[12] I. N. Stranski and L. Krastanow, Sitzungsber. Akad. Wiss. Wien. Math.-Naturwiss. **146**, 797 (1938).
[13] R. Loudon, *The Quantum Theory of Light* (Oxford University Press, Oxford, 2000).
[14] R. Hanbury-Brown and R. Q. Twiss, Nature (London) **177**, 27 (1956).
[15] R. v. Baltz, *Frontiers of Optical Spectroscopy*, NATO Science Series (Springer, Berlin, 2005).
[16] A. Gatti, E. Brambilla, M. Bache, and L. A. Lugiato, Phys. Rev. Lett. **93**, 093602 (2004).
[17] M. Malik, H. Shin, M. O'Sullivan, P. Zerom, and R. W. Boyd, Phys. Rev. Lett. **104**, 163602 (2010).
[18] D. Huang *et al.*, Science **254**, 1178 (1991).
[19] R. Glauber, Phys. Rev. Lett. **10**, 84 (1963).
[20] D. B. Scarl, Phys. Rev. **175**, 1661 (1968).
[21] F. Boitier, A. Godard, E. Rosencher, and C. Fabre, Nat. Phys. **5**, 267 (2009).
[22] B. R. Mollow, Phys. Rev. **175**, 1555 (1968).
[23] J. M. Roth, T. E. Murphy, and C. Xu, Opt. Lett. **27**, 2076 (2002).
[24] K. Mogi, K. Naganuma, and H. Yamada, Jpn. J. Appl. Phys. **27**, 2078 (1988).
[25] M. Blazek, S. Breuer, T. Gensty, W. Elsäßer, M. Hopkinson, K. M. Groom, M. Calligaro, P. Resneau, and M. Krakowski, Proc. SPIE **6603**, 66031Y (2007).
[26] D. F. Walls, Nature (London) **280**, 451 (1979).
[27] D. F. Walls, Nature (London) **306**, 141 (1983).
[28] H. J. Kimble, M. Dagenais, and L. Mandel, Phys. Rev. Lett. **39**, 691 (1977).
[29] M. Blazek, S. Hartmann, A. Molitor, and W. Elsäßer, Opt. Lett. **36**, 3455 (2011).
[30] Y.-C. Xin, A. Martinez, T. Saiz, A. J. Moscho, Y. Li, T. A. Nilsen, A. L. Gray, and L. F. Lester, IEEE Photon. Technol. Lett. **19**, 501 (2007).
[31] A. E. Zhukov, V. M. Ustinov, A. Y. Egorov, A. R. Kovsh, A. F. Tsatsul'nikov, N. N. Ledentsov, S. V. Zaitsev, N. Y. Gordeev, P. S. Kop'ev, and Z. I. Alferov, Jpn. J. Appl. Phys. **36**, 4216 (1997).
[32] H. Huang and D. G. Deppe, IEEE J. Quantum Electron. **37**, 691 (2001).
[33] S. Shin, U. Sharma, H. Tu, W. Jung, and S. A. Boppart, IEEE Photon. Technol. Lett. **22**, 1057 (2010).